This is a repository copy of *Microscale size effects in piezomagnetic material for the anti-plane problem*.

Article:

ORIGINAL PAPER

**Mingxiu Xu · Harm Askes · Xinchun Shang ·
Inna M. Gitman**

Microscale size effects in piezomagnetic material for the anti-plane problem

Abstract A continuum model of piezomagnetic material with strain, magnetic and piezomagnetic coupling gradient effects is proposed using a variational principle in this work. This model is employed to an anti-plane problem, and a general solution is constructed in polar coordinates. Special attention is paid to microstructural effects on the magnetic and mechanical response in an infinite piezomagnetic medium with a void. It is found that the microstructural length scales have a significant influence on the mechanic and magnetic fields. The three length scales (corresponding to strain, magnetic and piezomagnetic coupling gradients) are indispensable to describe the nonlocal effects of piezomagnetism. Additionally, controlling the direction and magnitude of the magnetic field at the edge of the void can be achieved by adjusting the microstructural length scales of the piezomagnetic medium.

Keywords   Piezomagnetic material · Microstructure · Strain gradient · Magnetic field gradient · Anti-plane problem

1 Introduction

Piezomagnetic components have important applications in many areas, including sensors, head recorders, micro-electro-mechanical systems (MEMS), ultrasonic generators, magneto-mechanical transducers, active vibration damping system, high-precision linear motors, micro-valves and micro-positioning devices [1, 2, 3]. With increasing levels of miniaturisation of structures and systems, the underlying microstructure of the material needs to be accounted for in modelling approaches for accurate and reliable descriptions and predictions of the mechanic and magnetic behaviour of these structures and systems. An effective modelling approach is to enrich the governing piezomagnetic continuum equations with additional terms that are envisaged to capture the microstructural effects. Such efforts may be inspired by gradient-enriched elasticity theories, in which the length scale parameters that accompany these higher-order gradient terms can typically be linked to the microstructural properties [4].

In this way, magneto-mechanical coupling has been combined with couple stress theory in [5, 6], with strain gradient theory in [7], with Eringen's stress-gradient theory in [8, 9], with Eringen's gradient theory adding inertia gradients in [10, 11] and with both strain and stress gradients in [12, 13]. However, in these

M. Xu · X. Shang
Department of Applied Mechanics, School of Mathematics and Physics, University of Science and Technology Beijing, Beijing 100083, China

H. Askes (✉)
Department of Civil and Structural Engineering, The University of Sheffield, Sheffield S1 3JD, UK
e-mail: h.askes@sheffield.ac.uk

I. M. Gitman
Department of Mechanical Engineering, The University of Sheffield, Sheffield S1 3JD, UK

applications, the length scales included in the model appear in the mechanical contributions only. Because the magnetic contributions have been shown to be equally sensitive to the microstructure of the material [14], microstructural terms in the magnetic parameters should be added for a more accurate description of magnetic parameters. Gradient enrichment of the magnetic induction is considered in [15, 16] and higher-order gradients of the magnetic field are added in [17, 18, 19, 20] based on Eringen's gradient theory, using the same scale parameters as those of the mechanical field.

For a more versatile description of magneto-mechanical coupling behaviour, a general piezomagnetic continuum model with gradients of strain, magnetic field and piezomagnetic coupling terms is used here, and the individual effects of three length scales on the removal of singularities from magnetic field and mechanical field and the prediction of size-dependent piezomagnetic response are discussed in detail using the finite element method [21]. In this paper, we will analyse the influence of the three length scales on the nonlocal effects of mechanic field and magnetic field in the context of the anti-plane boundary value problem using an analytical solution method.

2 Formulation of the piezomagnetic continuum model with gradients of strain, magnetic field and piezomagnetic coupling

2.1 Variational principle for a piezomagnetic medium

Consider a piezomagnetic body occupying a domain Ω with boundary Γ. The total energy functional I of the body in statics can be written as

$$I = \int_\Omega W\left(\varepsilon_{ij}, \varepsilon_{ij,k}, H_i, H_{i,j}\right)\mathrm{d}\Omega - V$$

$$= \int_\Omega W\left(\varepsilon_{ij}, \varepsilon_{ij,k}, H_i, H_{i,j}\right)\mathrm{d}\Omega - \int_\Omega \overline{f}_i u_i \mathrm{d}\Omega - \oint_\Gamma \left(\overline{t}_i u_i + \overline{p}_i \mathrm{D}u_i + \overline{\rho}\varphi + \overline{\pi}\mathrm{D}\varphi\right)\mathrm{d}S \tag{1}$$

where V is the work done, W is the internal energy density function, ε_{ij} is the strain, H_i is the magnetic field, u_i is the displacement field, φ is the magnetic potential and $\overline{f}_i$ is the body force [21].

The internal energy density includes the *standard* piezomagnetic contributions in terms of strain and magnetic field, but also *non-standard* contributions in terms of the spatial derivatives of strain and magnetic field (each of which will be discussed in specific detail below). In the same spirit, and motivated by the work of Sladek et al. on the work done by external "force" [7], the surface integral in V contains the external loading terms with $\overline{t}_i, \overline{p}_i, \overline{\rho}$ and $\overline{\pi}$ denoting the traction, the double traction, the magnetic traction and the magnetic double traction, respectively. Furthermore, we use the normal surface gradient operator $\mathrm{D}u_i = n_l u_{i,l}$ and $\mathrm{D}\varphi = n_l \varphi_{,l}$, with n_l being the component of outward unit normal vector on Γ.

Finally, the kinematic relationships relate the strain and magnetic field to the primary unknowns, that is the displacements u_i and the magnetic potential φ, according to

$$\begin{cases} \varepsilon_{ij} = \frac{1}{2}\left(u_{i,j} + u_{j,i}\right) \\ H_i = -\varphi_{,i} \end{cases}. \tag{2}$$

According to the Helmholtz principle of minimum energy dissipation, the total energy functional I should satisfy the variational equation

$$\delta I = \int_\Omega \delta W\left(\varepsilon_{ij}, \varepsilon_{ij,k}, H_i, H_{i,j}\right)\mathrm{d}\Omega - \int_\Omega \overline{f}_i \delta u_i \mathrm{d}\Omega$$

$$- \oint_\Gamma \left(\overline{t}_i \delta u_i + \overline{p}_i \mathrm{D}\delta u_i + \overline{\rho}\delta\varphi + \overline{\pi}\mathrm{D}\delta\varphi\right)\mathrm{d}S = 0 \tag{3}$$

Applying the Gauss formula, the following result is obtained:

$$\delta I = -\int_\Omega \left[\left(\frac{\partial W}{\partial \epsilon_{ij}}\right)_{,j} - \left(\frac{\partial W}{\partial \epsilon_{ij,k}}\right)_{,jk} + \overline{f}_i\right]\delta u_i d\Omega + \int_\Omega \left[\left(\frac{\partial W}{\partial H_i}\right)_{,i} - \left(\frac{\partial W}{\partial H_{i,j}}\right)_{,ij}\right]\delta\varphi d\Omega$$

$$+ \oint_\Gamma \left[\left(\frac{\partial W}{\partial \epsilon_{ij}} - \frac{\partial W}{\partial \epsilon_{ij,k}} \right)_{,k} n_j - \left(\frac{\partial W}{\partial \epsilon_{ij,k}} n_k \right)_{,j} + \left(\frac{\partial W}{\partial \epsilon_{ij,k}} n_k n_l \right)_{,l} n_j - \bar{t}_i \right] \delta u_i dS$$

$$+ \oint_\Gamma \left[-\left(\frac{\partial W}{\partial H_i} - \left(\frac{\partial W}{\partial H_{i,j}} \right)_{,j} \right) n_i + \left(n_j \frac{\partial W}{\partial H_{i,j}} \right)_{,i} - \left[\left(n_j \frac{\partial W}{\partial H_{i,j}} \right) n_l \right]_{,l} n_i - \bar{\rho} \right] \delta \varphi dS$$

$$+ \oint_\Gamma \left(\frac{\partial W}{\partial \varepsilon_{ij,k}} n_k n_j - \bar{p}_i \right) (\delta u_i)_{,l} n_l dS - \oint_\Gamma \left(n_i n_j \frac{\partial W}{\partial H_{i,j}} - \bar{\pi} \right) (\delta \varphi)_{,l} n_l dS = 0 \tag{4}$$

2.2 Constitutive relations and boundary conditions

We introduce the standard stress tensor t_{ij}, double stress tensor s_{ijk}, dipole magnetic flux density b_i and quadrupole magnetic flux density π_{ij} through the following relations:

$$\begin{cases} t_{ij} = \frac{\partial W}{\partial \varepsilon_{ij}} \\ s_{ijk} = \frac{\partial W}{\partial \varepsilon_{ij,k}} \\ b_i = -\frac{\partial W}{\partial H_i} \\ \pi_{ij} = -\frac{\partial W}{\partial H_{i,j}} \end{cases} \tag{5}$$

With the above definitions, the total stress σ_{ij} and total magnetic flux density B_i are

$$\begin{cases} \sigma_{ij} = t_{ij} - s_{ijk,k} \\ B_i = b_i - \pi_{ij,j} \end{cases} \tag{6}$$

Taking into account that the variations of δu_i and $\delta \varphi$ are arbitrary, we can extract the following equilibrium equations in Ω,

$$\begin{cases} \sigma_{ij,j} + \overline{f}_i = 0 \\ B_{i,i} = 0 \end{cases} \tag{7}$$

and the following boundary conditions on Γ

$$\begin{cases} (t_{ij} - s_{ijk,k}) n_j - (s_{ijk} n_k)_{,j} + (s_{ijk} n_k n_l)_{,l} n_j = \bar{t}_i \text{ or } u_i = \bar{u}_i \\ s_{ijk} n_k n_j = \bar{p}_i \text{ or } u_{i,l} n_l = \frac{\partial \bar{u}_i}{\partial \boldsymbol{n}} \\ (b_i - \pi_{ij,j}) n_i + [(\pi_{ij} n_j + \pi_i) n_l]_{,l} n_i - (\pi_{ij} n_j + \pi_i)_{,i} = \bar{\rho} \text{ or } \varphi = \overline{\varphi} \\ \pi_{ij} n_j n_i = \bar{\pi} \text{ or } n_l \varphi_{,l} = \frac{\partial \overline{\varphi}}{\partial \boldsymbol{n}} \end{cases} \tag{8}$$

The internal energy density function W includes gradients of strain, magnetic field and coupling terms, as shown in [21]:

$$W(\varepsilon_{ij}, \varepsilon_{ij,k}, H_i, H_{i,j}) = \frac{1}{2} \varepsilon_{ij} C_{ijkl} \varepsilon_{kl} + \frac{1}{2} \varepsilon_{ij,m} l_1^2 C_{ijkl} \varepsilon_{kl,m} - \varepsilon_{ij} q_{ijk} H_k$$

$$- \varepsilon_{ij,m} l_2^2 q_{ijk} H_{k,m} - \frac{1}{2} H_i \mu_{ij} H_j - \frac{1}{2} H_{i,m} l_3^2 \mu_{ij} H_{j,m} \tag{9}$$

In the above equations, C_{ijkl}, q_{ijk} and μ_{ij} are, respectively, elastic, piezomagnetic and magnetic permeability coefficients, whereas l_1, l_2 and l_3 are material length scale parameters reflecting microscale size effects, owing to the introduction of strain gradient, piezomagnetic coupling gradient and magnetic field gradient, respectively, in the energy function.

Substituting Eqs. (9) and (5) into Eq. (6), the following gradient-enriched constitutive equations can be obtained

$$\begin{cases} \sigma_{ij} = C_{ijkl} (\varepsilon_{kl} - l_1^2 \nabla^2 \varepsilon_{kl}) - q_{ijk} (H_k - l_2^2 \nabla^2 H_k) \\ B_i = q_{ijk} (\varepsilon_{jk} - l_2^2 \nabla^2 \varepsilon_{jk}) + \mu_{ij} (H_j - l_3^2 \nabla^2 H_j) \end{cases} \tag{10}$$

where $\nabla^2 \equiv \nabla^{\mathrm{T}}.\nabla$ is the Laplace operator.

Combining the kinematic equation Eq. (2), equilibrium equation Eq. (7) and constitutive equation Eq. (10) yields the following gradient-enriched governing equations in terms of the primary unknowns u_i and φ:

$$\begin{cases} C_{ijkl}(u_{k,jl} - l_1^2\nabla^2 u_{k,jl}) + q_{ijk}(\varphi_{,jk} - l_2^2\nabla^2\varphi_{,jk}) + \overline{f}_i = 0 \\ q_{ijk}(u_{i,jk} - l_2^2\nabla^2 u_{i,jk}) - \mu_{ij}(\varphi_{,ij} - l_3^2\nabla^2\varphi_{,ij}) = 0 \end{cases} \tag{11}$$

3 Analytical solution of anti-plane problems of piezomagnetic medium

3.1 *Construction of the solution* via *superposition*

Consider a transversely isotropic piezomagnetic material polarized along the z-direction and with the xy-plane as the plane of isotropy. Let the material be subjected to anti-plane shear strain and in-plane magnetic field H_x at infinity. Thus, the anti-plane displacements are described by

$$u_x = u_y = 0, u_z = w(x, y), \varphi = \varphi(x, y) \tag{12}$$

The non-vanishing strain and magnetic field components are

$$\begin{Bmatrix} \varepsilon_{zx} \\ \varepsilon_{zy} \end{Bmatrix} = \nabla w, \begin{Bmatrix} H_x \\ H_y \end{Bmatrix} = -\nabla\varphi \tag{13}$$

Substituting them into the gradient-enriched constitutive Eq. (10), where $C = \begin{bmatrix} c_{44} & \\ & c_{44} \end{bmatrix}$, $Q = \begin{bmatrix} q_{15} & \\ & q_{15} \end{bmatrix}$, $P = \begin{bmatrix} \mu_{11} & \\ & \mu_{11} \end{bmatrix}$, the total stress and total magnetic flux density can be obtained as

$$\begin{Bmatrix} \sigma_{zx} \\ \sigma_{zy} \end{Bmatrix} = c_{44}[\nabla w - l_1^2\nabla(\nabla^2 w)] + q_{15}[\nabla\varphi - l_2^2\nabla(\nabla^2\varphi)] \tag{14a}$$

$$\begin{Bmatrix} B_x \\ B_y \end{Bmatrix} = q_{15}[\nabla w - l_2^2\nabla(\nabla^2 w)] - \mu_{11}[\nabla\varphi - l_3^2\nabla(\nabla^2\varphi)] \tag{14b}$$

In the absence of body forces, substitution of Eqs. (12) and (13) into Eq. (11) leads to the following gradient-enriched governing equations:

$$\begin{cases} c_{44}(\nabla^2 w - l_1^2\nabla^2\nabla^2 w) + q_{15}(\nabla^2\varphi - l_2^2\nabla^2\nabla^2\varphi) = 0 \\ q_{15}(\nabla^2 w - l_2^2\nabla^2\nabla^2 w) - \mu_{11}(\nabla^2\varphi - l_3^2\nabla^2\nabla^2\varphi) = 0 \end{cases} \tag{15}$$

Equation (15) can be rewritten by factorizing the various derivatives as

$$\begin{cases} c_{44}(1 - l_1^2\nabla^2)\nabla^2 w + q_{15}(1 - l_2^2\nabla^2)\nabla^2\varphi = 0 \\ q_{15}(1 - l_2^2\nabla^2)\nabla^2 w - \mu_{11}(1 - l_3^2\nabla^2)\nabla^2\varphi = 0 \end{cases} \tag{16}$$

with the first solution set satisfying

$$\begin{cases} \nabla^2 w = 0 \\ \nabla^2\varphi = 0 \end{cases} \tag{17}$$

or rewritten as

$$\begin{cases} \nabla^2\{c_{44}(w - l_1^2\nabla^2 w) + q_{15}(\varphi - l_2^2\nabla^2\varphi)\} = 0 \\ \nabla^2\{q_{15}(w - l_2^2\nabla^2 w) - \mu_{11}(\varphi - l_3^2\nabla^2\varphi)\} = 0 \end{cases} \tag{18}$$

and the second solution set satisfying

$$\begin{cases} c_{44}(w - l_1^2\nabla^2 w) + q_{15}(\varphi - l_2^2\nabla^2\varphi) = 0 \\ q_{15}(w - l_2^2\nabla^2 w) - \mu_{11}(\varphi - l_3^2\nabla^2\varphi) = 0 \end{cases} \tag{19}$$

The total solution of Eq. (15) is the combination of the first solution set obtained from Eq. (17) and the second solution set obtained from Eq. (19).

3.2 *Solution in polar coordinates*

The two solutions sets are solved in polar coordinates with $\nabla^2 = \frac{\partial^2}{\partial r^2} + \frac{1}{r}\frac{\partial}{\partial r} + \frac{1}{r^2}\frac{\partial^2}{\partial \theta^2}$, assuming $w = f(r)\cos(n\theta)$, $\varphi = g(r)\cos(n\theta)$. The solution of Eq. (17) is

$$\begin{cases} w_1 = a_0 + h_0 lnr + \sum_{n=1}^{\infty}\left(a_n r^n + h_n r^{-n}\right)\cos n\theta \\ \varphi_1 = c_0 + d_0 lnr + \sum_{n=1}^{\infty}\left(c_n r^n + d_n r^{-n}\right)\cos n\theta \end{cases} \tag{20}$$

where a_n, h_n, c_n and d_n are undetermined constants. Substituting $w = f(r)\cos(n\theta)$, $\varphi = g(r)\cos(n\theta)$ into Eq. (19) and dividing by $\cos n\theta$, the following equations are obtained:

$$\begin{cases} c_{44}\left[1 - l_1^2\left(\frac{d^2}{dr^2} + \frac{1}{r}\frac{d}{dr} - \frac{n^2}{r^2}\right)\right]f(r) + q_{15}\left[1 - l_2^2\left(\frac{d^2}{dr^2} + \frac{1}{r}\frac{d}{dr} - \frac{n^2}{r^2}\right)\right]g(r) = 0 \\ q_{15}\left[1 - l_2^2\left(\frac{d^2}{dr^2} + \frac{1}{r}\frac{d}{dr} - \frac{n^2}{r^2}\right)\right]f(r) - \mu_{11}\left[1 - l_3^2\left(\frac{d^2}{dr^2} + \frac{1}{r}\frac{d}{dr} - \frac{n^2}{r^2}\right)\right]g(r) = 0 \end{cases} \tag{21}$$

Introduce the modified Bessel function $\left(\frac{d^2}{dx^2} + \frac{1}{x}\frac{d}{dx} - \frac{n^2}{x^2}\right)y(x) = y(x)$ and let $x = r\sqrt{\lambda}$, then the modified Bessel function is

$$\left(\frac{d^2}{dr^2} + \frac{1}{r}\frac{d}{dr} - \frac{n^2}{r^2}\right)y\left(r\sqrt{\lambda}\right) = \lambda y\left(r\sqrt{\lambda}\right) \tag{22}$$

Based on Eq. (22), substitute $f(r) = \alpha_1 I_n\left(r\sqrt{\lambda}\right)$, $g(r) = \alpha_2 I_n\left(r\sqrt{\lambda}\right)$ into Eq. (21a), by which the following equation is obtained

$$c_{44}\left(1 - l_1^2\lambda\right)\alpha_1 + q_{15}\left(1 - l_2^2\lambda\right)\alpha_2 = 0 \tag{23a}$$

Next, substituting $f(r) = \alpha_1 K_n\left(r\sqrt{\lambda}\right)$, $g(r) = \alpha_2 K_n\left(r\sqrt{\lambda}\right)$ into Eq. (21b) leads to

$$q_{15}\left(1 - l_2^2\lambda\right)\alpha_1 - \mu_{11}\left(1 - l_3^2\lambda\right)\alpha_2 = 0 \tag{23b}$$

where I_n and K_n are modified Bessel functions of order n of the first and second kind, with α_1 and α_2 undetermined constants.

In order to obtain a non-trivial solution $[\alpha_1, \alpha_2]$, λ should satisfy

$$\det\begin{vmatrix} c_{44}\left(1 - l_1^2\lambda\right) & q_{15}\left(1 - l_2^2\lambda\right) \\ q_{15}\left(1 - l_2^2\lambda\right) & -\mu_{11}\left(1 - l_3^2\lambda\right) \end{vmatrix} = 0 \tag{24}$$

Letting $\beta_1 = \frac{q_{15}^2}{C_{44}\mu_{11}}$ and $\beta_2 = l_1^2 l_3^2 + l_2^4\frac{q_{15}^2}{C_{44}\mu_{11}}$ leads to the following inequalities

$$\begin{cases} \left(l_1^2 - l_3^2\right)^2 + 4\beta_1\left(l_1^2 l_2^2 + l_2^2 l_3^2 - l_1^2 l_3^2 - l_2^4\right) > 0 \\ \frac{\left(l_1^2 + l_3^2\right) + 2l_2^2\beta_1}{\beta_2} > 0 \\ \frac{1 + \beta_1}{\beta_2} > 0 \end{cases} \tag{25}$$

There are two positive eigenvalues λ_1 and λ_2, and two sets of $[\alpha_1, \alpha_2]$ corresponding to λ_1 and λ_2, respectively:

$$\lambda_{1,2} = \frac{\left(l_1^2 + l_3^2\right) + 2l_2^2\beta_1 \pm \sqrt{\left(l_1^2 - l_3^2\right)^2 + 4\beta_1\left(l_1^2 l_2^2 + l_2^2 l_3^2 - l_1^2 l_3^2 - l_2^4\right)}}{2\beta_2} \tag{26}$$

$$\begin{cases} \alpha_1^{(1)} = \beta_1 \\ \alpha_2^{(1)} = \frac{\beta_1 q_{15}\left(1 - l_2^2\lambda_1\right)}{\mu_{11}\left(1 - l_3^2\lambda_1\right)} \end{cases} \tag{27a}$$

$$\begin{cases} \alpha_1^{(2)} = \beta_1 \\ \alpha_2^{(2)} = \frac{\beta_1 q_{15}\left(1 - l_2^2\lambda_2\right)}{\mu_{11}\left(1 - l_3^2\lambda_2\right)} \end{cases} \tag{27b}$$

Thus, the solutions $f(r)$ and $g(r)$ in Eq. (21) are

$$
\begin{bmatrix} f_n(r) \\ g_n(r) \end{bmatrix} = G_{1n} \begin{bmatrix} \alpha_1^{(1)} \\ \alpha_2^{(1)} \end{bmatrix} I_n\left(\sqrt{\lambda_1}r\right) + G_{2n} \begin{bmatrix} \alpha_1^{(2)} \\ \alpha_2^{(2)} \end{bmatrix} I_n\left(\sqrt{\lambda_2}r\right)
$$
$$
+ G_{3n} \begin{bmatrix} \alpha_1^{(1)} \\ \alpha_2^{(1)} \end{bmatrix} K_n\left(\sqrt{\lambda_1}r\right) + G_{4n} \begin{bmatrix} \alpha_1^{(2)} \\ \alpha_2^{(2)} \end{bmatrix} K_n\left(\sqrt{\lambda_2}r\right)
$$

(28)

where G_{1n}, G_{2n}, G_{3n} and G_{4n} are undetermined constants. Therefore, the solution of Eq. (19) reads

$$
\begin{cases}
w_2 = \sum_{n=0}^{\infty}\left[G_{1n}\alpha_1^{(1)}I_n\left(\sqrt{\lambda_1}r\right) + G_{2n}\alpha_1^{(2)}I_n\left(\sqrt{\lambda_2}r\right) + G_{3n}\alpha_1^{(1)}K_n\left(\sqrt{\lambda_1}r\right) + G_{4n}\alpha_1^{(2)}K_n\left(\sqrt{\lambda_2}r\right)\right]\cos n\theta \\
\varphi_2 = \sum_{n=0}^{\infty}\left[G_{1n}\alpha_2^{(1)}I_n\left(\sqrt{\lambda_1}r\right) + G_{2n}\alpha_2^{(2)}I_n\left(\sqrt{\lambda_2}r\right) + G_{3n}\alpha_2^{(1)}K_n\left(\sqrt{\lambda_1}r\right) + G_{4n}\alpha_2^{(2)}K_n\left(\sqrt{\lambda_2}r\right)\right]\cos n\theta
\end{cases}
$$

(29)

The expressions of displacements w and φ are

$$
\begin{cases}
w = w_1 + w_2 = a_0 + h_0 \ln r + \sum_{n=1}^{\infty}(a_n r^n + h_n r^{-n})\cos n\theta \\
\quad + \sum_{n=0}^{\infty}\left[G_{1n}\alpha_1^{(1)}I_n\left(\sqrt{\lambda_1}r\right) + G_{2n}\alpha_1^{(2)}I_n\left(\sqrt{\lambda_2}r\right) + G_{3n}\alpha_1^{(1)}K_n\left(\sqrt{\lambda_1}r\right) + G_{4n}\alpha_1^{(2)}K_n\left(\sqrt{\lambda_2}r\right)\right]\cos n\theta \\
\varphi = \varphi_1 + \varphi_2 = c_0 + d_0 \ln r + \sum_{n=1}^{\infty}(c_n r^n + d_n r^{-n})\cos n\theta \\
\quad + \sum_{n=0}^{\infty}\left[G_{1n}\alpha_2^{(1)}I_n\left(\sqrt{\lambda_1}r\right) + G_{2n}\alpha_2^{(2)}I_n\left(\sqrt{\lambda_2}r\right) + G_{3n}\alpha_2^{(1)}K_n\left(\sqrt{\lambda_1}r\right) + G_{4n}\alpha_2^{(2)}K_n\left(\sqrt{\lambda_2}r\right)\right]\cos n\theta
\end{cases}
$$

(30)

The various stress and magnetic flux measures can be expressed in polar coordinates as follows

$$
\varepsilon_{zr} = \frac{\partial w}{\partial r}
$$
$$
\varepsilon_{z\theta} = \frac{1}{r}\frac{\partial w}{\partial \theta}
$$
$$
t_{zr} = C_{44}\frac{\partial w}{\partial r} + q_{15}\frac{\partial \varphi}{\partial r}
$$
$$
t_{z\theta} = \frac{C_{44}}{r}\frac{\partial w}{\partial \theta} + \frac{q_{15}}{r}\frac{\partial \varphi}{\partial \theta}
$$
$$
s_{zrr} = C_{44}l_1^2\left(\frac{\partial^2 w}{\partial r^2}\right) + q_{15}l_2^2\left(\frac{\partial^2 \varphi}{\partial r^2}\right)
$$
$$
s_{z\theta\theta} = C_{44}l_1^2\frac{1}{r^2}\left(\frac{\partial^2 w}{\partial \theta^2}\right) + q_{15}l_2^2\frac{1}{r^2}\left(\frac{\partial^2 \varphi}{\partial \theta^2}\right)
$$
$$
\sigma_{zr} = C_{44}\left[\frac{\partial w}{\partial r} - l_1^2\frac{\partial}{\partial r}\left(\nabla^2 w\right)\right] + q_{15}\left[\frac{\partial \varphi}{\partial r} - l_2^2\frac{\partial}{\partial r}\left(\nabla^2 \varphi\right)\right]
$$
$$
\sigma_{z\theta} = C_{44}\left[\frac{1}{r}\frac{\partial w}{\partial \theta} - l_1^2\frac{1}{r}\frac{\partial}{\partial \theta}\left(\nabla^2 w\right)\right] + q_{15}\left[\frac{1}{r}\frac{\partial \varphi}{\partial \theta} - l_2^2\frac{1}{r}\frac{\partial}{\partial \theta}\left(\nabla^2 \varphi\right)\right]
$$
$$
H_r = -\frac{\partial \varphi}{\partial r}
$$
$$
H_\theta = -\frac{1}{r}\frac{\partial \varphi}{\partial \theta}
$$

$$b_r = -\mu_{11}\frac{\partial\varphi}{\partial r} + q_{15}\frac{\partial w}{\partial r}$$

$$b_\theta = -\frac{\mu_{11}}{r}\frac{\partial\varphi}{\partial\theta} + \frac{q_{15}}{r}\frac{\partial w}{\partial\theta}$$

$$\pi_{rr} = q_{15}l_2^2\left(\frac{\partial^2 w}{\partial r^2}\right) - \mu_{11}l_3^2\left(\frac{\partial^2\varphi}{\partial r^2}\right)$$

$$\pi_{\theta\theta} = q_{15}l_2^2\frac{1}{r^2}\left(\frac{\partial^2 w}{\partial\theta^2}\right) - \mu_{11}l_3^2\frac{1}{r^2}\left(\frac{\partial^2\varphi}{\partial\theta^2}\right)$$

$$B_r = q_{15}\left[\frac{\partial w}{\partial r} - l_2^2\frac{\partial}{\partial r}(\nabla^2 w)\right] - \mu_{11}\left[\frac{\partial\varphi}{\partial r} - l_3^2\frac{\partial}{\partial r}(\nabla^2\varphi)\right]$$

$$B_\theta = q_{15}\left[\frac{1}{r}\frac{\partial w}{\partial\theta} - l_2^2\frac{1}{r}\frac{\partial}{\partial\theta}(\nabla^2 w)\right] - \mu_{11}\left[\frac{1}{r}\frac{\partial\varphi}{\partial\theta} - l_3^2\frac{1}{r}\frac{\partial}{\partial\theta}(\nabla^2\varphi)\right] \tag{31}$$

3.3 Several special cases

Next, we will briefly discuss the nature of the solutions for several special cases that will be studied in detail in the next Section.

Case 1: $l_1 = l_2 = l_3 = 0$.
In this case, there is no solution for Eq. (19), and the expressions of displacements w and φ are

$$\begin{cases} w = a_0 + h_0\ln r + \sum_{n=1}^{\infty}\left(a_n r^n + h_n r^{-n}\right)\cos n\theta \\ \varphi = c_0 + d_0\ln r + \sum_{n=1}^{\infty}\left(c_n r^n + d_n r^{-n}\right)\cos n\theta \end{cases} \tag{32}$$

Case 2: $l_3 = l_2 = 0, l_1 \neq 0$.
In this case, there is only one real eigenvalue $\lambda = (1 + \beta_1)/l_1^2$, and one set of $[\alpha_1, \alpha_2]$:

$$\begin{cases} \alpha_1 = 1/\beta_1 \\ \alpha_2 = C_{44}/q_{15} \end{cases} \tag{33}$$

Then, the solutions of $f(r)$ and $g(r)$ in Eq. (21) are

$$\begin{bmatrix} f_n(r) \\ g_n(r) \end{bmatrix} = G_{1n}\begin{bmatrix} \alpha_1 \\ \alpha_2 \end{bmatrix}I_n\left(\sqrt{\lambda}r\right) + G_{3n}\begin{bmatrix} \alpha_1 \\ \alpha_2 \end{bmatrix}K_n\left(\sqrt{\lambda}r\right) \tag{34}$$

by which the solution of Eq. (19) can be written as

$$\begin{cases} w_2 = \sum_{n=0}^{\infty}\left[G_{1n}\alpha_1 I_n\left(\sqrt{\lambda}r\right) + G_{3n}\alpha_1 K_n\left(\sqrt{\lambda}r\right)\right]\cos n\theta \\ \varphi_2 = \sum_{n=0}^{\infty}\left[G_{1n}\alpha_2 I_n\left(\sqrt{\lambda}r\right) + G_{3n}\alpha_2 K_n\left(\sqrt{\lambda}r\right)\right]\cos n\theta \end{cases} \tag{35}$$

where the expressions of displacements w and φ are

$$\begin{cases} w = a_0 + h_0\ln r + \sum_{n=1}^{\infty}\left(a_n r^n + h_n r^{-n}\right)\cos n\theta + \sum_{n=0}^{\infty}\left[G_{1n}\alpha_1 I_n\left(\sqrt{\lambda}r\right) + G_{3n}\alpha_1 K_n\left(\sqrt{\lambda}r\right)\right]\cos n\theta \\ \varphi = c_0 + d_0\ln r + \sum_{n=1}^{\infty}\left(c_n r^n + d_n r^{-n}\right)\cos n\theta + \sum_{n=0}^{\infty}\left[G_{1n}\alpha_2 I_n\left(\sqrt{\lambda}r\right) + G_{3n}\alpha_2 K_n\left(\sqrt{\lambda}r\right)\right]\cos n\theta \end{cases} \tag{36}$$

Case 3: $l_1 = l_2 = 0, l_3 \neq 0$.
In this case, there is only one real eigenvalue $\lambda = (1 + \beta_1)/l_3^2$, and one set of $[\alpha_1, \alpha_2]$:

$$\begin{cases} \alpha_1 = \beta_1 \\ \alpha_2 = -\dfrac{q_{15}}{\mu_{11}} \end{cases} \tag{37}$$
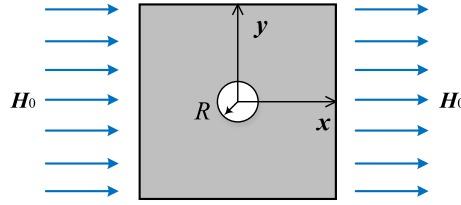
Fig.1 An infinite piezomagnetic medium with a circular microvoid

Table 1 Material parameters of MSCP and MEE [22]

Material name		MSCP	MEE
Elastic constant [GPa]	C_{44}	13.6	43
Piezomagnetic constant [N/Am]	q_{15}	-60.9	550
Magnetic permeability [10^{-4} Ns^2/C^2]	μ_{11}	0.054	0.05

The solution is the same as Case 2.

Case 4: $l_1 = l_2 = l_3 = l \neq 0$.

In this case, there is only one real eigenvalue $\lambda = 1/l^2$, and one set of $[\alpha_1, \alpha_2]$. And α_1, α_2 in Eq. (23) have no correlation. The solution is the same as Case 2.

Thus, we have a consistent set of solutions for the above 4 special cases, consisting of the solution to the standard equations of piezomagnetics given in Eq. (32) augmented with additional terms due to gradient enrichment as given via the last terms in Eq. (36). It is therefore sufficient to assess the quantitative and qualitative effects of the length scales from the investigation of Eq. (36). However, to show the additional effect of l_3 on magnetic field, another special case is considered too.

Case 5: $l_2 = 0, l_3 = kl_1 \neq 0$.

In this case, k should satisfy $k \geq \sqrt{1 + \sqrt{4\beta_1}}$ or $k \leq \sqrt{1 - \sqrt{4\beta_1}}$ according to Eq. (25), while the expressions of displacements w and φ are shown in Eq. (30).

4 Analysis

4.1 Computational example

Consider a circular microvoid in an infinite piezomagnetic medium, as shown in Fig. 1 but see also [23]. The radius of the void is $R = 2$ mm. A transversely isotropic magneto-electro-elastic (MEE) material and a (Terfenol-D)-epoxy mixed component (MSCP) have been chosen. Assuming the material is polarized along the $z(3)$-direction and has the $xy(12)$-plane as its plane of isotropy, the relevant material parameters are listed in Table 1. The specimen is subjected to a uniform anti-plane shear strain $\varepsilon_{xz} = \varepsilon_0 = 0.0005$ and in-plane magnetic field $H_0 = 200$ A/m. Therefore, the far-field conditions are

$$\begin{cases} \varphi^{(M)} = -H_0 x = -H_0 r \cos\theta \\ w^{(M)} = \varepsilon_0.x = \varepsilon_0.r\cos\theta \end{cases} (r \to \infty) \tag{38}$$

Based on the results of Sect. 3.2 and the symmetry of loading, the displacement and magnetic potential in the matrix are

$$w^{(M)} = \left(a_1 r + h_1 r^{-1}\right)\cos\theta + \left[G_{31}\alpha_1^{(1)}K_1\left(\sqrt{\lambda_1}r\right) + G_{41}\alpha_1^{(2)}K_1\left(\sqrt{\lambda_2}r\right)\right]\cos\theta \tag{39a}$$

$$\varphi^{(M)} = \left(c_1 r + d_1 r^{-1}\right)\cos\theta + \left[G_{31}\alpha_2^{(1)}K_1\left(\sqrt{\lambda_1}r\right) + G_{41}\alpha_2^{(2)}K_1\left(\sqrt{\lambda_2}r\right)\right]\cos\theta \tag{39b}$$

while the displacement and magnetic potential in the void are given by

$$w^{(V)} = 0 \tag{40a}$$

$$\varphi^{(V)} = m_1 r \cos\theta \tag{40b}$$

The superscripts M and V indicate the matrix and the void, respectively, whereas a_1, h_1, c_1, d_1, G_{31}, G_{41} and m_1 are unknown coefficients.

The boundary conditions at the interface $r = R$ can be obtained according to Eq. (8):

$$\begin{cases} \varphi(R^-) = \varphi(R^+) \\ B_r(R^-) = B_r(R^+) \\ \sigma_{zr}(R^+) = 0 \\ s_{zrr}(R^+) = 0 \\ \pi_{rr}(R^+) = 0 \end{cases} \tag{41}$$

Combining with the far-field conditions, 7 unknown coefficients in Eq. (39) and (40) can be determined. For several special cases, $w^{(M)}$, $\varphi^{(M)}$ and the boundary conditions are:

Case 1: $l_1 = l_2 = l_3 = 0$

$$w^{(M)} = (a_1 r + h_1 r^{-1})\cos\theta \tag{42a}$$

$$\varphi^{(M)} = (c_1 r + d_1 r^{-1})\cos\theta \tag{42b}$$

The 5 unknown coefficients a_1, h_1, c_1, d_1, and m_1 can be determined by the 2 far-field conditions and the following 3 boundary conditions:

$$\begin{cases} \varphi(R^-) = \varphi(R^+) \\ B_r(R^-) = B_r(R^+) \\ \sigma_{zr}(R^+) = 0 \end{cases} \tag{43}$$

Case 2: $l_3 = l_2 = 0, l_1 \neq 0$

$$w^{(M)} = \left[a_1 r + h_1 r^{-1} + G_{31}\alpha_1 K_1\left(\sqrt{\lambda}r\right)\right]\cos\theta \tag{44a}$$

$$\varphi^{(M)} = \left[c_1 r + d_1 r^{-1} + G_{31}\alpha_2 K_1\left(\sqrt{\lambda}r\right)\right]\cos\theta \tag{44b}$$

where $\lambda = (1 + \beta_1)/l_1^2$, $\alpha_1 = 1/\beta_1$, $\alpha_2 = \frac{C_{44}}{q_{15}}$. The 6 unknown coefficients a_1, h_1, c_1, d_1, G_{31}, and m_1 can be determined by the 2 far-field conditions and the following 4 boundary conditions:

$$\begin{cases} \varphi(R^-) = \varphi(R^+) \\ B_r(R^-) = B_r(R^+) \\ \sigma_{zr}(R^+) = 0 \\ s_{zrr}(R^+) = 0 \end{cases} \tag{45}$$

Further, combining Eqs. (14) and (44), the expressions of b_r, b_θ, π_{rr} and $\pi_{\theta\theta}$ in the matrix are:

$$b_r = \left[-\mu_{11}(c_1 - d_1 r^{-2}) + q_{15}(a_1 - h_1 r^{-2})\right]\cos\theta \tag{46a}$$

$$b_\theta = \left[\mu_{11}(c_1 + d_1 r^{-2}) - q_{15}(a_1 + h_1 r^{-2})\right]\sin\theta \tag{46b}$$

$$\pi_{rr} = 0 \tag{46c}$$

$$\pi_{\theta\theta} = 0 \tag{46d}$$

which show that the magnetic flux density (b_r, b_θ) and the quadrupole polarization (π_{rr}, $\pi_{\theta\theta}$) are independent of l_1.

Case 3: $l_1 = l_2 = 0, l_3 \neq 0$.

The expressions for w and φ are the same as in case 2, but with $\lambda = (1 + \beta_1)/l_3^2$, $\alpha_1 = \beta_1$, $\alpha_2 = -\frac{q_{15}}{\mu_{11}}$. Moreover, the 4 boundary conditions are:

$$\begin{cases} \varphi(R^-) = \varphi(R^+) \\ B_r(R^-) = B_r(R^+) \\ \sigma_{zr}(R^+) = 0 \\ \pi_{rr}(R^+) = 0 \end{cases} \tag{47}$$

Further, combining Eqs. (14) and (44), the expressions of t_{zr}, $t_{z\theta}$, s_{zrr} and $s_{z\theta\theta}$ in the matrix are:

$$t_{zr} = \left[c_{44}\left(a_1 - h_1 r^{-2}\right) + q_{15}\left(c_1 - d_1 r^{-2}\right)\right]\cos\theta \tag{48a}$$

$$t_{z\theta} = -\left[c_{44}\left(a_1 + h_1 r^{-2}\right) + q_{15}\left(c_1 + d_1 r^{-2}\right)\right]\sin\theta \tag{48b}$$

$$s_{zrr} = 0 \tag{48c}$$

$$s_{z\theta\theta} = 0 \tag{48d}$$

which show that the standard stresses (t_{zr}, $t_{z\theta}$) and the double stress (s_{zrr}, $s_{z\theta\theta}$) are independent of l_3.

Case 4: $l_1 = l_2 = l_3 = l \neq 0$

$$w^{(M)} = \left[a_1 r + h_1 r^{-1} + G_1 K_1\left(\sqrt{\lambda}r\right)\right]\cos\theta \tag{49a}$$

$$\varphi^{(M)} = \left[c_1 r + d_1 r^{-1} + G_2 K_1\left(\sqrt{\lambda}r\right)\right]\cos\theta \tag{49b}$$

where $\lambda = 1/l^2$, $G_1 = G_{31}\alpha_1$, $G_2 = G_{31}\alpha_2$. The 7 unknown coefficients a_1, h_1, c_1, d_1, G_1, G_2 and m_1 can be determined by the 2 far-field conditions and the 5 boundary conditions of Eq. (41).

Case 5: $l_2 = 0, l_3 = kl_1 \neq 0$.

$w^{(M)}, \varphi^{(M)}$ and the boundary conditions are shown in Eqs. (39) and (41), and the only additional requirement is that $k \geq \sqrt{1 + \sqrt{4\beta_1}}$ or $k \leq \sqrt{1 - \sqrt{4\beta_1}}$.

4.2 *Results and discussion*

The effects of the three length scales on the mechanic and magnetic fields will be discussed based on the simulation results next. Because the results of MEE material and MSCP material show similar patterns, principally, the results of MEE material are discussed in detail, while the results of MSCP material are given afterwards for supplementary insight.

Figure 2 shows the effect of all three length scales on the distribution of the strain ε in and around the void. Figure 2a1 and a2 show the case $l_1 \neq 0$ with $l_2 = l_3 = 0$, Fig. 2b1 and b2 show the case $l_3 \neq 0$ with $l_1 = l_2 = 0$, Fig. 2c1 and c2 show the case $l_1 = l_2 = l_3 = l$, and Fig. 2d1 and d2 show the case $l_2 = 0$ with $l_1 \neq 0$ and $l_3 \neq 0$.

An increase in value of l_1 (while initially keeping $l_1 = 0$) has a strong influence on the distribution of strain near the void, particularly the radial component as demonstrated in Fig. 2a1. For low values of l_1, the response is governed by the boundary conditions of the classical (non-gradient enriched) problem which dictate a zero radial shear strain on the edge of the void. For larger values of l_1, the boundary conditions imposed on stresses have less and less influence on the value of ε_{zr}. Conversely, the concentration of circumferential shear strain $\varepsilon_{z\theta}$ near the void decreases as l_1 increases, as Fig. 2a2 shows.

Figure 2b1 and b2 shows that, when $l_1=l_2=0$, the distribution of ε_{zr} and $\varepsilon_{z\theta}$ remain unchanged as l_3 increases, and in isolation l_3 appears to have no influence on the strains. On the other hand, there is a modest effect of l_3 on the strains when $l_1 \neq 0$: there is a minor perturbation of the distribution of ε_{zr} close to the edge with increasing values of l_3, as shown in Fig. 2d1. However, the overriding observation is that the effect of on l_3 the strains is minimal.

Next, we consider the case $l_1=l_2=l_3=l$. Fig. 2c1 and c2 shows the two relevant components ε_{zr} and $\varepsilon_{z\theta}$ for increasing value of the length scale. Compared to the case of only one non-zero length scale, i.e. $l_1 \neq 0$ while $l_2=l_3=0$ as shown in Fig. 2a1 and a2, having multiple non-zero length scales leads to much more pronounced smoothing of the strain profile—particularly for the radial shear strain component. Since we have demonstrated above that the strains hardly depend on l_3, we conclude that this increased smoothing of the strains is the added effect of l_2. It means that the piezomagnetic coupling length scale l_2 has a similar effect on the mechanical field as the mechanical field length scale l_1. The piezomagnetic coupling length scale l_2 has a quantitative contribution to the nonlocal mechanical response, but it is not indispensable in the smoothing of the mechanical field variables.

Figure 3 shows the effect of all three length scales on the distribution of the magnetic field in and around the void. Figure 3a1 and a2 show the case $l_1 \neq 0$ with $l_2=l_3=0$, Figure 3b1 and b2 show the case $l_3 \neq 0$ with $l_1=l_2=0$, Fig. 3c1 and c2 show the case $l_1=l_2=l_3=l$, while Fig. 3d1 and d2 show the case $l_2=0$ with $l_1 \neq 0$ and $l_3 \neq 0$.

(a1) $\theta = 0°, l_2 = l_3 = 0$

(a2) $\theta = -90°, l_2 = l_3 = 0$

(b1) $\theta = 0°, l_1 = l_2 = 0$

(b2) $\theta = -90°, l_1 = l_2 = 0$

(c1) $\theta = 0°, l_1 = l_2 = l_3 = l$

(c2) $\theta = -90°, l_1 = l_2 = l_3 = l$

(d1) $\theta = 0°, l_2 = 0, l_1 = 0.2$mm

(d2) $\theta = -90°, l_2 = 0, l_1 = 0.2$mm
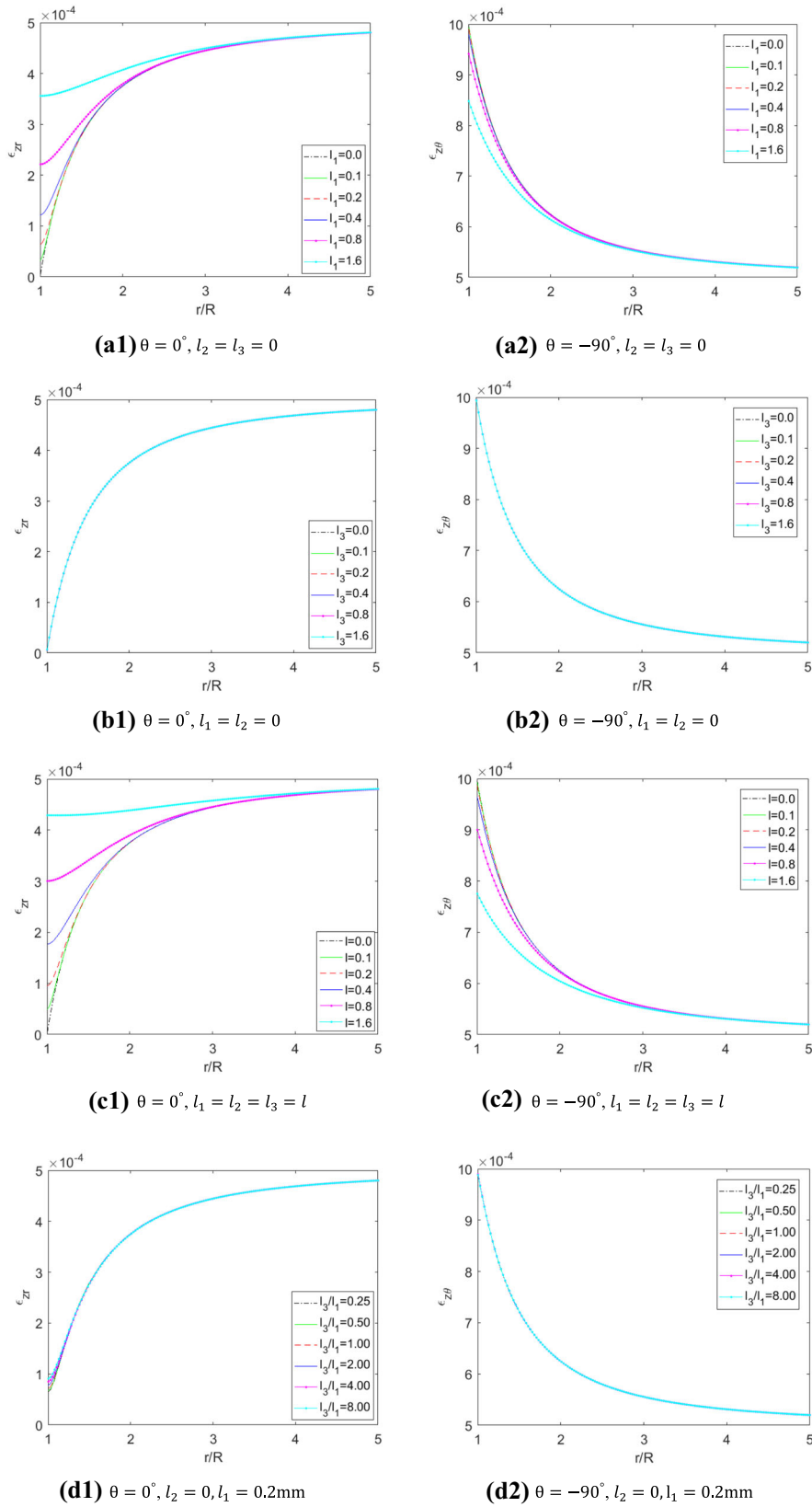
Fig. 2 The distribution of ε_{zr} and $\varepsilon_{z\theta}$ (MEE, unit of length scales: mm)

(a1) $\theta = 0°, l_2 = l_3 = 0$

(a2) $\theta = -90°, l_2 = l_3 = 0$

(b1) $\theta = 0°, l_1 = l_2 = 0$

(b2) $\theta = -90°, l_1 = l_2 = 0$

(c1) $\theta = 0°, l_1 = l_2 = l_3 = l$

(c2) $\theta = -90°, l_1 = l_2 = l_3 = l$

(d1) $\theta = 0°, l_2 = 0, l_1 = 0.2$mm

(d2) $\theta = -90°, l_2 = 0, l_1 = 0.2$mm
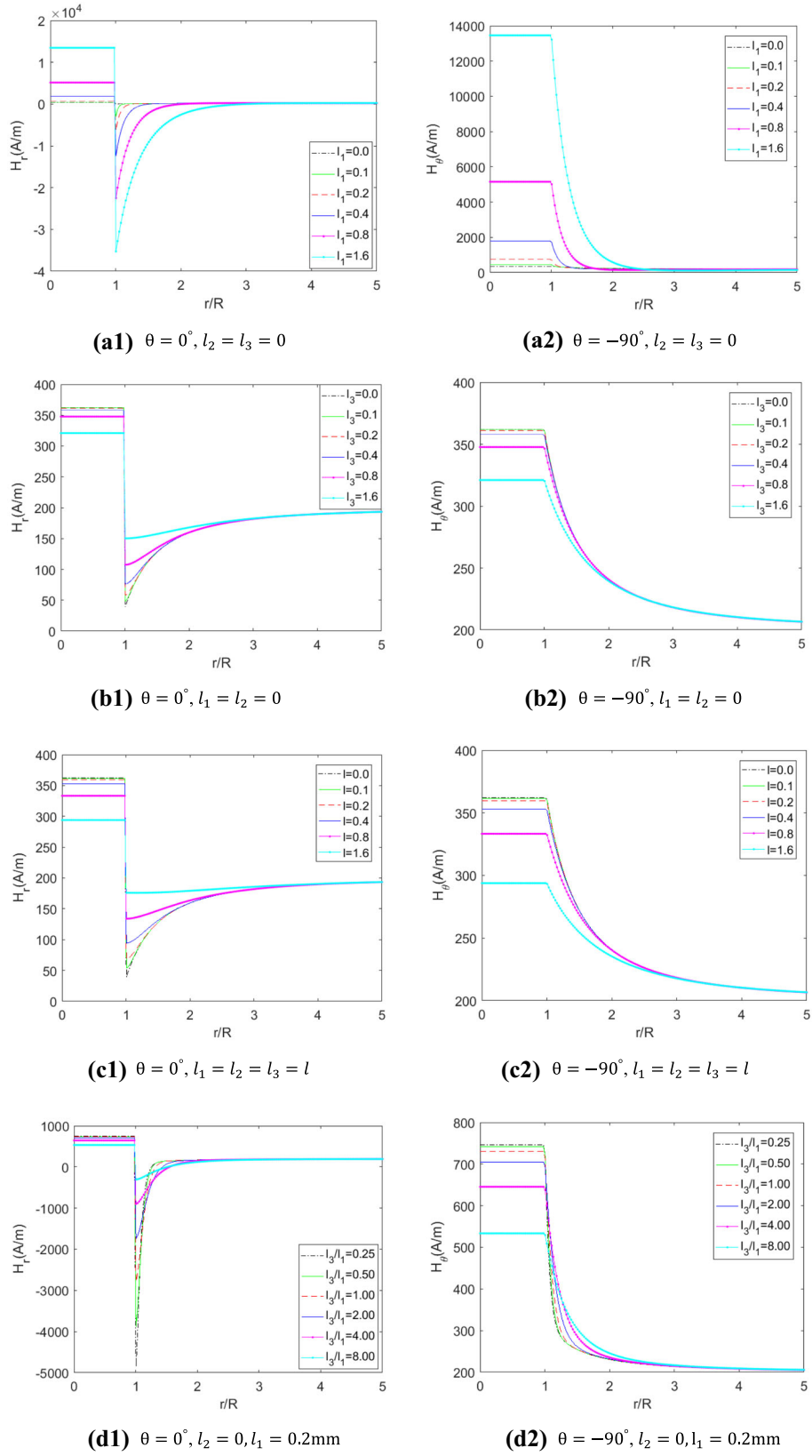
Fig. 3 The distribution of H_r and H_θ (MEE, unit of length scales: mm)
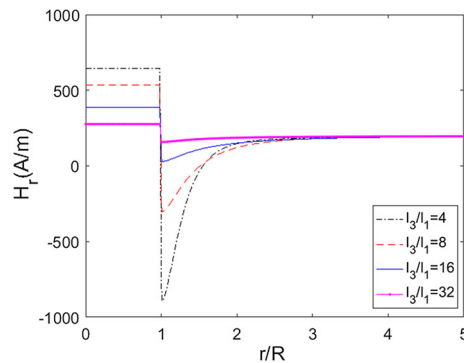
Fig. 4 The distribution of H_r along $\theta=0°$ when $l_2=0$ (MEE, unit of length scales: mm)

Taking only $l_1 \neq 0$, both the magnetic field in the void and around the void depart from the far-field value as l_1 increases, as Fig. 3a1 and a2 show. This goes against the usual observation that nonlocal effects decrease the concentration of the field variables near the void. On the other hand, taking $l_3 \neq 0$ as the only non-zero length scale, the magnetic field in the void and around the void approach the far-field value as l_3 increases, and the concentration of magnetic field near the void is decreased as l_3 increases, shown in Fig. 3b1, b2—a similar trend is observed taking both $l_1 \neq 0$ and $l_3 \neq 0$, as shown in Fig. 3d1, d2. Therefore, to describe the magnetic field realistically, the magnetic field gradient l_3 must be included.

Furthermore, the effect of l_3 on decreasing the concentration of magnetic field near the void is less pronounced than the combined effect l_1, l_2 and l_3 shown in Fig. 3c1, c2. It means that the piezomagnetic coupling length scale l_2 has a similar effect on the magnetic field as the magnetic field length scale l_3. Similar to its effect on the mechanical field l_2, has a quantitative contribution to the nonlocal magnetic response, but it is not indispensable in the magnetic field description.

The effects of three length scales on the mechanic field and magnetic field are summarised as follows: the strain gradient length scale l_1 in Eq. (10) alone can describe the nonlocal effect on the mechanical field, while the piezomagnetic coupling gradient l_2 has a quantitative contribution to the nonlocal mechanic response. However, the strain gradient l_1 in Eq. (10) alone cannot describe the nonlocal effect on the magnetic field; the magnetic field gradient l_3 must be included. Therefore, to describe the nonlocal effect of piezomagnetism comprehensively, the length scales accompanying the strain gradient and magnetic field gradients are indispensable, while the effect of the coupling length scale l_2 is quantitative only and certainly not essential.

l_1 and l_3 have effects on magnetic field in the void and around the void. It also shows that we can control the magnetic field in the void and around the void by adjusting the length scales (namely, designing the microstructures). In Fig. 4, with the increase in l_3/l_1, the direction of H_r changes. When l_3/l_1 is equal to 4 and 8, the value of H_r is negative, while it turns positive when l_3/l_1 is over 16. So, it is speculated that, at the edge of the void, $H_r=0$ can be obtained if l_3/l_1 takes certain value. Controlling the direction of magnetic field and zero magnetic field has a lot of practical application, such as in weak magnetic detection [24], bioelectromagnetics research [25] and low energy physics experiment research [26, 27]. So, it is meaningful for the study of these phenomena.

5 Conclusions

In this investigation, a model for piezomagnetic material with gradient effects of strain, magnetic and piezomagnetic coupling field is developed. An analytical solution for the anti-plane problem is constructed based on two sets of fundamental solutions that are superposed. In the analysis of an infinite piezomagnetic medium with a circular microvoid, it is found that the scale of microstructure has a significant influence on the mechanic field and magnetic field, and the length scales corresponding to strain and magnetic gradients are indispensable in order to describe the nonlocal effects of piezomagnetism. Especially, controlling the direction and magnitude of the magnetic field at the interface of the void can be achieved by tuning the ratio of void radius to microstructural length scales of the piezomagnetic medium.

References

1. Zhang, D.G., Li, M.H., Zhou, H.M.: A general one-dimension nonlinear magneto-elastic coupled constitutive model for magnetostrictive materials. AIP Adv. **5**, 107201 (2015)
2. Giannakopoulos, A.E., Parmaklis, A.Z.: The contact problem of a circular rigid punch on piezomagnetic materials. Int. J. Solids Struct. **44**(14–15), 4593–4612 (2007)
3. Zhou, Y.T., Kim, T.W.: Frictional moving contact over the surface between a rigid punch and piezomagnetic materials - Terfenol-D as example. Int. J. Solids Struct. **50**(24), 4030–4042 (2013)
4. Askes, H., Aifantis, E.C.: Gradient elasticity in statics and dynamics: An overview of formulations, length scale identification procedures, finite element implementations and new results. Int. J. Solids Struct. **48**(13), 1962–1990 (2011)
5. Arefi, M., Kiani, M.: Magneto-electro-mechanical bending analysis of three-layered exponentially graded microplate with piezomagnetic face-sheets resting on Pasternak's foundation via MCST. Mech. Adv. Mater. Struct. **27**(5), 383–395 (2020)
6. Arefi, M., Kiani, M., Zenkour, A.M.: Size-dependent free vibration analysis of a three-layered exponentially graded nano-/micro-plate with piezomagnetic face sheets resting on Pasternak's foundation via MCST. J. Sandw. Struct. Mater. **22**(1), 55–86 (2020)
7. Sladek, J., Sladek, V., Stanak, P., Pan, E.: FEM formulation for size-dependent theory with application to micro coated piezoelectric and piezomagnetic fiber-composites. Comput. Mech. **59**(1), 93–105 (2017)
8. Arefi, M., Zamani, M.H., Kiani, M.: Smart electrical and magnetic stability analysis of exponentially graded shear deformable three-layered nanoplate based on nonlocal piezo-magneto-elasticity theory. J. Sandw. Struct. Mater. **22**(3), 599–625 (2020)
9. Sadeghzadeh, S., Mahinzare, M.: Nonlocal strain gradient theory for dynamical modeling of a thermo-piezo-magnetically actuated spinning inhomogeneous nanoshell. *Mech. Based Des. Struct. Mach.* 1–22 (2020)
10. Chen, A.L., Yan, D.J., Wang, Y.S., Zhang, C.: In-plane elastic wave propagation in nanoscale periodic piezoelectric/piezomagnetic laminates. Int. J. Mech. Sci. **153–154**, 416–429 (2019)
11. Park, W.T., Han, S.C.: Buckling analysis of nano-scale magneto-electro-elastic plates using the nonlocal elasticity theory. Adv. Mech. Eng. **10**(8), 1–16 (2018)
12. Malikan, M., Van Bac, N., Tornabene, F.: Electromagnetic forced vibrations of composite nanoplates using nonlocal strain gradient theory. Mater. Res. Express, **5**(7) (2018)
13. Arefi, M., Kiani, M., Rabczuk, T.: Application of nonlocal strain gradient theory to size dependent bending analysis of a sandwich porous nanoplate integrated with piezomagnetic face-sheets. Compos. Part B Eng. **168**(February), 320–333 (2019)
14. Chikazumi, S.: Physics of Ferromagnetism. Physics (College. Park. Md) **1**(11), 655 (1997)
15. Gholami, R., Ansari, R., Gholami, Y.: Size-dependent bending, buckling and vibration of higher-order shear deformable magneto-electro-thermo-elastic rectangular nanoplates. Mater. Res. Express **4**(6), 065702 (2017)
16. Ke, L.L., Wang, Y.S., Yang, J., Kitipornchai, S.: The size-dependent vibration of embedded magneto-electro-elastic cylindrical nanoshells. Smart Mater. Struct. **23**(12), 125036 (2014)
17. Sahmani, S., Aghdam, M.M.: Nonlocal strain gradient shell model for axial buckling and postbuckling analysis of magneto-electro-elastic composite nanoshells. Compos. Part B Eng. **132**, 258–274 (2018)
18. Ma, L.H., Ke, L.L., Reddy, J.N., Yang, J., Kitipornchai, S., Wang, Y.S.: Wave propagation characteristics in magneto-electro-elastic nanoshells using nonlocal strain gradient theory. Compos. Struct. **199**, 10–23 (2018)
19. Ebrahimi, F., Dabbagh, A.: Wave dispersion characteristics of rotating heterogeneous magneto-electro-elastic nanobeams based on nonlocal strain gradient elasticity theory. J. Electromagn. Waves Appl. **32**(2), 138–169 (2018)
20. Ebrahimi, F., Dabbagh, A: Nonlocal strain gradient based wave dispersion behavior of smart rotating magneto-electro-elastic nanoplates. Mater. Res. Express ,**4**(2), 025003 (2017)
21. Xu, M., Gitman, I.M., Askes, H.: A gradient-enriched continuum model for magneto-elastic coupling: Formulation, finite element implementation and in-plane problems. Comput. Struct. **212**, 275–288 (2019)
22. Daga, A., Ganesan, N., Shankar, K.: Comparative studies of the transient response for PECP, MSCP, Barium Titanate, magneto-electro-elastic finite cylindrical shell under constant internal pressure using finite element method. Finite Elem. Anal. Des. **44**, 89–104 (2008)
23. Yue, Y.M., Xu, K.Y., Aifantis, E.C.: Microscale size effects on the electromechanical coupling in piezoelectric material for anti-plane problem. Smart Mater. Struct. **23**, 125043 (2014)
24. Kotsiaros, S., Olsen, N.: End-to-End simulation study of a full magnetic gradiometry mission. Geophys. J. Int. **196**(1), 100–110 (2013)
25. P. R. Malmivuo J, *Bioelectromagnetism: Principles and Applications of Bioelectric and Biomagnetic Fields*. 1995.
26. Pendlebury, J.M., et al.: Revised experimental upper limit on the electric dipole moment of the neutron. Phys. Rev. D - Part. Fields, Gravit. Cosmol. **92**(9), 1–23 (2015)
27. Tayler, M.C.D., et al.: Invited Review Article: Instrumentation for nuclear magnetic resonance in zero and ultralow magnetic field. Rev. Sci. Instrum. **88**(9), 091101 (2017)